

PAPER • OPEN ACCESS

## Detonation properties of hydrazine nitrate

To cite this article: A V Utkin *et al* 2019 *J. Phys.: Conf. Ser.* **1147** 012034

View the [article online](#) for updates and enhancements.



**IOP | ebooks™**

Bringing together innovative digital publishing with leading authors from the global scientific community.

Start exploring the collection—download the first chapter of every title for free.

# Detonation properties of hydrazine nitrate

A V Utkin, V M Mochalova, S I Torunov, V A Sosikov, V A Garanin  
and L B Romanova

Institute of Problems of Chemical Physics of the Russian Academy of Sciences, Academician  
Semenov Avenue 1, Chernogolovka, Moscow Region 142432, Russia

E-mail: [utkin@icp.ac.ru](mailto:utkin@icp.ac.ru)

**Abstract.** The results of investigation of the detonation waves structure, the critical diameter, detonation parameters and the dependence of detonation velocity on the charge diameter for pressed hydrazine nitrate (HN) charges in the density range of 1.40–1.68 g/cm<sup>3</sup> are presented. It was found that the critical diameter drops with the initial density decrease. Under steady-state detonation conditions at an initial density of 1.68 g/cm<sup>3</sup>, a high detonation velocity of 8.92 km/s is observed in HN charges. The change of the detonation velocity with variation of the initial density is not monotonous, but has a characteristic s-shape.

## 1. Introduction

Hydrazine nitrate (HN) N<sub>2</sub>H<sub>4</sub>HNO<sub>3</sub> has been studied in detail and its physicochemical properties are given, for example, in [1–8]. The use of HN as one of the components of rocket fuels [8–12] requires the determination of their detonation parameters, critical detonation conditions. However, the available data on the detonation properties of HN are extremely limited and they are sometimes ambiguous, what is most clearly manifested in the character of the dependence of the detonation velocity  $D$  on the initial density  $\rho_0$ . According to experimental data [13],  $D$  reaches a maximum value of 5.64 km/s at  $\rho_0 = 1.3$  g/cm<sup>3</sup> while detonation velocities exceeding 8.5 km/s at  $\rho_0 = 1.6$  g/cm<sup>3</sup> have been obtained in [8, 14]. Furthermore, there are no existing data on the detonation wave structures and the critical diameter. This work is devoted to an experimental investigation of these issues.

## 2. Experimental scheme and results

In the experiments, the velocity of HN–water boundary was recorded by VISAR interferometer. Figure 1 shows the scheme of the experiments on study of detonation waves structure. Pressed HN charges with an initial density in the range of 1.4–1.68 g/cm<sup>3</sup> were used. Samples were prepared by pressing an HN powder with an average particle size of about 500  $\mu$ m, which shape is close to the cubic one. The charge consists of three samples of HN, the thickness of each of being equal to the radius. To initiate detonation in HN the plane wave generator and the pressed charge of the desensitized RDX were used. A laser beam was reflected from aluminum foil with a thickness of 400  $\mu$ m, that was placed between the end of the charge and the water window. To determine the absolute value of the velocity, two interferometers with velocity fringe constants of 280 and 1280 m/s were used simultaneously. Using the ionization gauge, the detonation velocity was measured in each experiment.



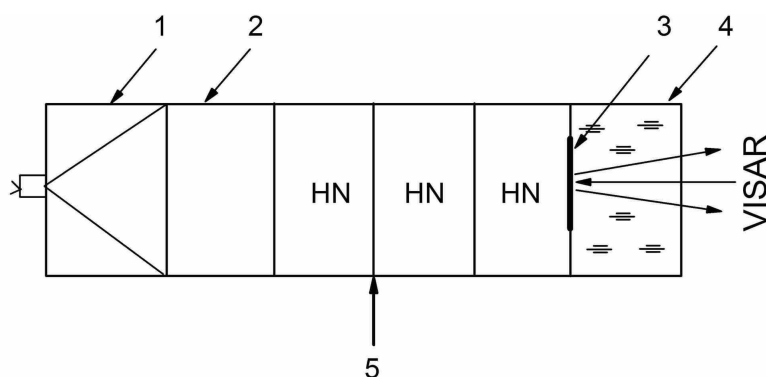


**Figure 1.** Scheme of experiments for investigation of the reaction zone structure of steady-state detonation waves in HN: 1—the plane wave generator; 2—the pressed charge of the desensitized RDX; 3—aluminum foil; 4—the water window; 5—the ionization gauge.

**Table 1.** Detonation parameters of HN.

| No | $\rho_0$ (g/cm <sup>3</sup> ) | $D$ (km/s)      | $u_{CJ}$ (km/s) | $P_{CJ}$ (GPa) |
|----|-------------------------------|-----------------|-----------------|----------------|
| 1  | 1.415                         | $5.59 \pm 0.05$ | $0.63 \pm 0.03$ | $5.0 \pm 0.2$  |
| 2  | 1.50                          | $6.12 \pm 0.05$ | $0.96 \pm 0.03$ | $8.8 \pm 0.3$  |
| 3  | 1.55                          | $7.67 \pm 0.05$ | $1.05 \pm 0.03$ | $14.5 \pm 0.3$ |
| 4  | 1.64                          | $8.80 \pm 0.05$ | $1.45 \pm 0.03$ | $21.1 \pm 0.4$ |
| 5  | 1.68                          | $8.92 \pm 0.05$ | $1.63 \pm 0.03$ | $24.4 \pm 0.4$ |
| 6  | 1.68                          | $8.92 \pm 0.05$ | $1.63 \pm 0.03$ | $24.4 \pm 0.4$ |

The particle velocity profiles for the HN samples with initial density of 1.4–1.68 g/cm<sup>3</sup> are shown in figures 2 and 3. The values of an initial density of the samples, the detonation velocity  $D$ , the particle velocity  $u_{CJ}$  and the  $P_{CJ}$  pressure at the Chapman–Jouguet (CJ) point at the charge diameter of 40 mm (except number 5, where the charge diameter is 60 mm) are shown in table 1. The parameters of the CJ point were calculated on the basis of the measured particle velocity profiles and  $D$ . At the same time, the unloading isentrope of the explosion products was approximated by the polytropic  $PV^n = \text{const}$ . The designation of the velocity profiles in figures 2 and 3 and the numbers of the experiments in table 1 are the same.

At an initial density of 1.64 g/cm<sup>3</sup> and higher, the structure of the velocity profiles has a shape that is typical of pressed explosives [15]. The velocity behind the shock jump decreases, and the von Neumann spike is recorded in the reaction zone. A sharp increase in the velocity at a time of 100 ns is due to the circulation of waves in the aluminum foil. The end of the reaction zone and the transition to the unloading wave (the CJ point position) on the velocity profiles is not noticeable, and there are certain difficulties in estimating the character of the reaction time. To solve this problem, in this case, the approach proposed in previous research [16] is realized, which is based on a comparison of velocity profiles obtained for charges of different diameters. If the detonation parameters remain constant, the flow in the reaction zone does not depend on the diameter, whereas in the unloading wave the flow changes, what makes it possible to determine the position of the CJ point.

The particle velocity profiles with density of 1.64 and 1.68 g/cm<sup>3</sup> for different charge diameters are shown in figure 2. In experiment 4, the initial density is 1.64 g/cm<sup>3</sup> and charge diameter is

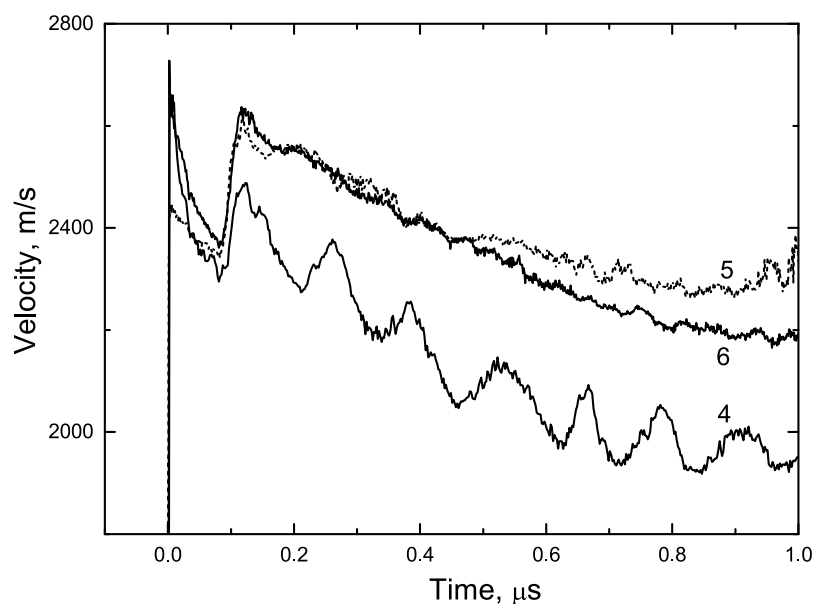


**Figure 2.** Particle velocity profiles on the HN–water boundary at different densities: 4—1.64; 5, 6—1.68 g/cm<sup>3</sup>.

40 mm. In experiments 5 and 6 at the initial density of 1.68 g/cm<sup>3</sup>, the diameters change from 60 to 40 mm, while the detonation velocity is the same. The velocity profiles at the border with the window also coincide, at least in the range from 0.1 to 0.5  $\mu$ s. A noticeable discrepancy is due to the influence of the charge diameter on the velocity gradient in the unloading wave which begins at large time values. This suggests that the characteristic reaction time is approximately 0.5  $\mu$ s. It is noteworthy that immediately after the shock jump, the amplitude values of the von Neumann spike in experiments 5 and 6 do not coincide, which is due to the reproducibility of the experimental results. This is confirmed by comparison of results of different experiments with the same diameters and the initial densities of the charges. In this case velocity profiles coincide with good accuracy.

A decrease in the initial density of HN charges not only results in the decrease of absolute values of the particle velocity, but also changes the characteristics of the dependence of velocity on time. Directly behind the shock wave, the von Neumann spike is still recorded, which is much less pronounced than in experiments with high density. Moreover, the velocity is constant or oscillates near the mean value (figure 3) during the entire recording time. The absence of the influence of the unloading wave, which should reduce the parameters outside the reaction zone, may be due to the increase in reaction time, because the CJ point moves to later times. However, this then means that the flow in the reaction zone, the duration of which exceeds 1  $\mu$ s, does not correspond to the classical detonation model, according to which there is a decrease of particle velocity during the chemical reaction.

The measured values of the detonation velocity as a function of the initial density, with a charge diameter of 40 mm, are shown in figure 4. A distinctive feature of the obtained results is a sharp increase of  $D$  in the density range of 1.5–1.6 g/cm<sup>3</sup>. Moreover, this effect is not a consequence of the influence of the charge diameter on the detonation velocity. This is evidenced by the data on the dependence of the detonation velocity on the charge diameter, according to which the detonation velocity is a constant at diameters of 40 mm and greater. This gives reason to believe that the measured value  $D = 8.92$  km/s is the maximum and corresponds to ideal detonation. Reduction of the charge diameter up to 30 mm results in a marked decrease

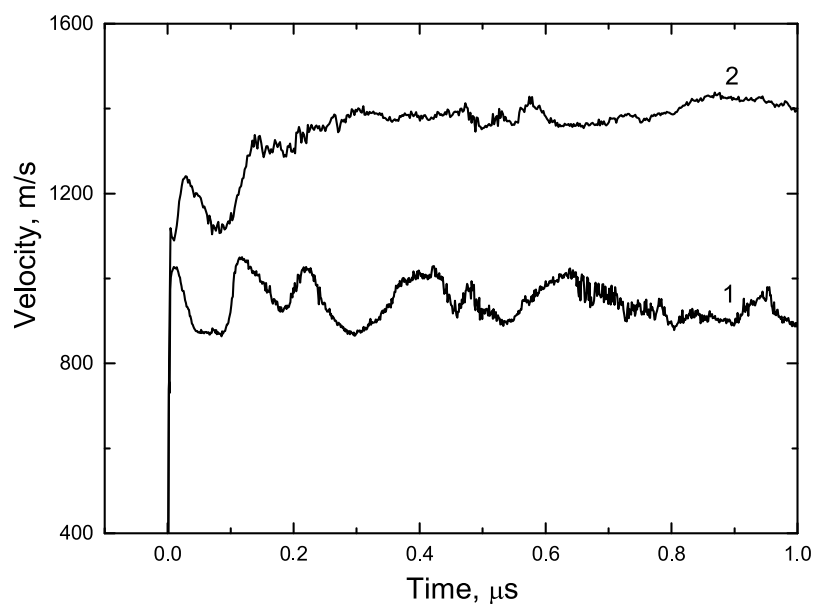


**Figure 3.** Particle velocity profiles on the HN–water boundary at different densities of charge: 1—1.415; 2—1.50 g/cm<sup>3</sup>.

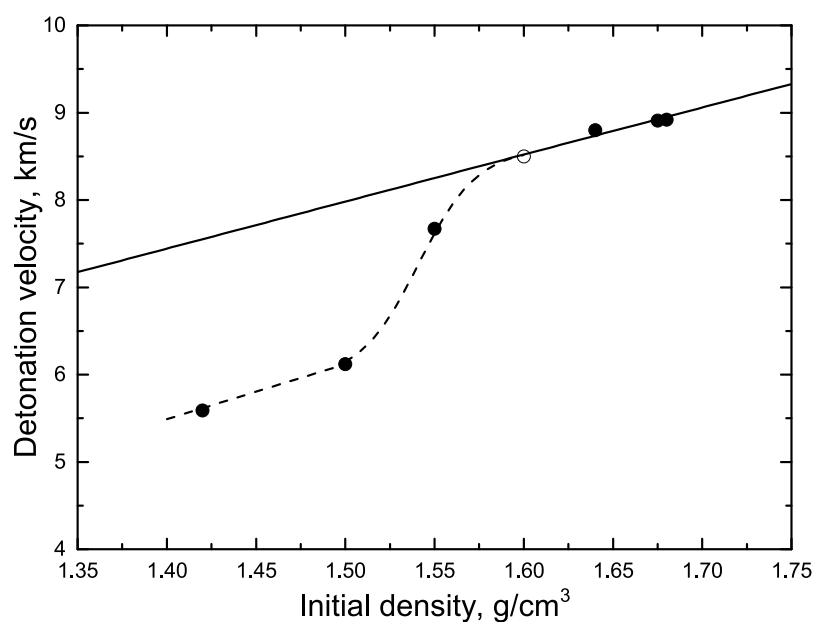


**Figure 4.** The dependence of detonation velocity on the initial density of HN. The open circle relates to previously published data [8, 14].

of the detonation velocity, and at 20 mm the detonation attenuates. The velocity profiles at the HN–water boundary also change accordingly. Thus, the critical diameter of HN with a density of 1.68 g/cm<sup>3</sup> is greater than 20 mm, but less than 30 mm.

An analogous detonation velocity dependence on the charge diameter is also observed at a density of 1.55 g/cm<sup>3</sup>. In this case, detonation attenuates at a diameter of 15 mm, whereas at a diameter of 20 mm or more a steady-state detonation regime is established. With a decrease

of the charge diameter from 40 to 20 mm the velocity profiles are qualitatively similar and only absolute values of the particle velocity decrease. At the same time, with a charge diameter of 15 mm, the time dependence changes qualitatively, the von Neumann spike disappears and the velocity increases monotonically after the shock jump, i.e., the critical diameter at a density of  $1.55 \text{ g/cm}^3$  is greater than 15 mm, but less than 20 mm.

### 3. Discussion

Results of the experiments show that the detonation properties of HN have a number of features. Under steady-state detonation conditions at an initial density of  $1.68 \text{ g/cm}^3$ , a high detonation velocity of  $8.92 \text{ km/s}$  is observed in HN charges. The pressure at the CJ point does not exceed  $25 \text{ GPa}$ , which corresponds to the value of the polytropic index close to 4.5.

The change of the detonation velocity with variation of the initial density is not monotonous, but has a characteristic s-shape:  $D$  increases sharply with increasing  $\rho_0$  in the range of  $1.5\text{--}1.6 \text{ g/cm}^3$  (figure 4). Such a dependence of  $D(\rho_0)$  does not allow us to relate HN to the second group of high explosives, as has been suggested in previous research [17], since the data given in figure 4 were obtained with a fixed charge diameter and should lie either on the linear dependence  $D(\rho_0)$  (ideal detonation), or on the dependence with the maximum, which was observed in previous research [14] for HN charges with a diameter of  $41.4 \text{ mm}$ . Such a significant discrepancy between the experimental data is probably due either to the structure of the investigated samples (for example, the particle size) or to the conditions for the undertaking of experiments. It is also noteworthy that the dependence  $D = a\rho_0 - b$ , where  $a = 5.388 \text{ km cm}^3/(\text{s g})$ ,  $b = 0.100 \text{ km/s}$ , which has been proposed in previous research [14] for the ideal detonation of HN and is shown by the solid line in figure 4, agrees well with the results of the present work at  $\rho_0 > 1.6 \text{ g/cm}^3$ .

Despite the complex character of the obtained  $D(\rho_0)$  dependence, it is not a unique feature of HN. A similar characteristic of the detonation velocity change with the initial density variation was observed in previous research [18] for nitroguanidine. In the interval of  $1.30\text{--}1.62 \text{ g/cm}^3$ , the experimental data for nitroguanidine lie on the  $D(\rho_0)$  dependence corresponding to the ideal detonation, but at  $\rho_0 < 1.2 \text{ g/cm}^3$  the detonation velocity  $D$  decreases sharply, and in previous research [18] this has been related to the realization of the low-velocity detonation regime. It is probable that a similar regime is realized in HN at  $\rho_0 < 1.5 \text{ g/cm}^3$ . Low-velocity detonation is observed for many types of condensed energy materials, including liquid and solid high explosives [19]. Steady-state propagation of detonation with low velocity is observed for certain values of the particle size of high explosive and the charge diameter. In the present work, we used HN with a sufficiently large crystalline particle size (approximately  $0.5 \text{ mm}$ ), which probably explains the difference between the obtained dependence  $D(\rho_0)$  and some results of previous research [14].

### 4. Conclusion

With respect to the example of nitroguanidine, it has been demonstrated [18] that in different intervals of the initial density, the properties of high explosives can correspond to different groups of explosives. This conclusion also applies to HN, whose critical diameter increases with initial density increase, at least for  $\rho_0 \geq 1.55 \text{ g/cm}^3$ , which is typical for high explosives of the 2nd group.

### Acknowledgments

This work is supported by program of the Presidium of the Russian Academy of Sciences No. 56 “The fundamental principles of breakthrough technologies in the interests of national security”.

### References

- [1] Audrieth L F and Ogg B A 1951 *The Chemistry of Hydrazine* (New York: Wiley)

- [2] Khmelniyskiy L I 1962 *Handbook of High Explosives* (Moscow: Military Artillery Engineering Academy of Dzerzhinsky)
- [3] Sarner S F 1966 *Propellant Chemistry* (Madison: Reinhold)
- [4] Liu J 2015 *Liquid Explosives* (Berlin: Springer)
- [5] Klapötke T M, Rienäcker C M and Zewen H 2002 *Nitrate Anorg. Allg. Chem.* **628** 2372–4
- [6] Robinson R J and McCrone W C 1958 *Anal. Chem.* **30** 1014–5
- [7] Shklovskiy A A, Semishin V I and Simutin V I 1960 *J. Appl. Chem.* **33** 1411–3
- [8] Miron Y and Perlee H E 1974 The hard start phenomena in hypergolic engines *Report CR-140361* (NASA)
- [9] Urbana L F A and Ryker D W 1960 Fuel *Patent* United States Patent Office 2943927
- [10] Haury V E and Golding D R V 1974 Solid propellant containing fuel-oxidizer component prepared from fused oxidizers *Patent* United States Patent Office 3837938
- [11] Paine T and Thompson W W 1978 Inhibited solid propellant composition containing beryllium *Patent* United States Patent Office 4111729
- [12] Bruenner R S, Oberth A E, Clark G M and Katakian A 1998 Liquid nitrate oxidizer compositions *Patent* United States Patent Office 5734124
- [13] Medard L 1952 *Meml. Poudres* **34** 147–57
- [14] Price D, Liddiard T P and Drosd R D 1966 The detonation behavior of hydrazine mononitrate *Report NOLTR-66-31* (U.S. Naval Ordnance Lab.)
- [15] Utkin A V, Kolesnikov S A and Pershin S V 2002 *Combust., Explos. Shock Waves* **38** 590–7
- [16] Mochalova V M, Utkin A V and Lapin S M 2016 *Combust., Explos. Shock Waves* **52** 329–34
- [17] Price D 1967 Contrasting patterns in the behavior of high explosives *Symp. (Int.) on Combustion* vol 11 pp 693–702
- [18] Price D and Clairmont A R 1969 Explosive behavior of nitroguanidine *Symp. (Int.) on Combustion* vol 12 pp 761–70
- [19] Belyaev A F, Bobolev V K, Korotkov A I, Sulimov A A and Chuiko S V 1973 *Transition of Combustion to Detonation for Condensed Systems* (Moscow: Nauka)